Robotica (2003) volume 21, pp. 335–340. © 2003 Cambridge University Press
DOI: 10.1017/S0263574703005010 Printed in the United Kingdom

Path design of redundant flexible robot manipulators to reduce residual vibration in the presence of obstacles

Kyung-Jo Park

Division of Mechanical and Automotive Engineering, Yosu National University, Yosu, Chonnanm, 550–749 (South Korea)

(Received in Final Form: November 11, 2002)

SUMMARY

A method is presented for generating the path that significantly reduces residual vibration of the redundant, flexible robot manipulator in the presence of obstacles. The desired path is optimally designed so that the system completes the required move with minimum residual vibration, avoiding obstacles. The dynamic model and optimal path are effectively formulated and computed by using a special moving coordinate, called VLCS, to represent the link flexibility. The path to be designed is developed by a combined Fourier series and polynomial function to satisfy both the convergence and boundary condition matching problems. The concept of correlation coefficients is used to select the minimum number of design variables. A planar three-link manipulator is used to evaluate this method. Results show that residual vibration can be drastically reduced by selecting an appropriate path, in the presence of obstacles.

KEYWORDS: Path design; Residual vibration; Obstacles; Redundant manipulators.

1. INTRODUCTION

Most industrial robots in use today are composed of heavy and stiff links to satisfy the required repeatability and accuracy. Light, flexible robot arms offer, on the other hand, significant advantages over the heavy and stiff robot arms. They consume less energy, are safer, and can move faster.[1] Their main disadvantage and the reason they are not widely used – is precisely their flexibility that gives rise to major residual vibrations and arm tip oscillations.

Internal, material damping will typically be light, and the addition of passive external dampers would impede the dynamic response of the arm, offsetting the advantages gained by the light structure. Thus, some form of active vibration damping is required to achieve satisfactory performance, and ideally the 'active' component would be the existing actuator. A further complication is that, in general, the dynamic response of the arm cannot be predicted, because it depends strongly on the load mass which may be unknown or variable, and the precise position of the arm tip may be difficult to ascertain.

Many strategies exist for the control of such systems. Book[2] reviewed a number of approaches including feedback and feed-forward control, passive damping enhancement, and structural design strategies. Karolov and Chen[3] developed a control scheme for a single-link flexible robot arm which is robust to variations in the system natural frequencies. A number of authors used simplified, multi-degree-of-freedom, lumped parameter systems to model multi-axis flexible robot arms. Meckl and Seering[4,5] explored open-loop control of such systems using a 'bang-bang' control function, and a control function constructed to avoid exciting resonance of the system. They also examined the performance of a control function based on a ramped sinusoid function. This work was further developed by Singhose et al.[6] who used input shaping by a sequence of impulses to improve the performance of the control system. Yamada and Nakagawa[7] proposed a method of reducing residual vibration caused by variations in the natural frequency of a single degree of freedom system, while Vincent et al.[8] developed a two-stage control algorithm for lumped parameter systems. Stage one is an open-loop rapid positioning phase, while stage two consists of a closed-loop damping phase. Jayasuriya and Choura[9] developed an open-loop forcing function based on minimum energy which eliminates residual vibration while making response time small. Recently William and Donogh[10] proposed a method to design an actuator required to position the remote load and, simultaneously to provide active vibration damping by absorbing the reflected waves.

In contrast to the above researches based on the lumped parameter model, there exist many researches to reduce the vibration of the arm tip by using continuum mechanics. Asada et al.[11] proposed a method to suppress the tracking error of the arm tip by using the inverse dynamics. Parks[12,13] has shown that the residual vibration can be reduced by designing path itself. In other words, from an initial point to a final point, there exist countless paths through which the endpoint of the arm can pass. Among these, we can select one path that minimizes the residual vibration by using an appropriate method. This approach is beneficial to avoiding the obstacles, including both the fixed and moving ones, because it designs the path itself.

Meanwhile redundant manipulators have been studied extensively because the existence of redundant degrees of freedom enables them to avoid both the singular point and the obstacles effciently.[14–16] Compared with the non-redundant manipulators, there exist, however, some problems when we analyze the dynamic response, or design the path of the redundant manipulators. The dimensionality is increased, so we cannot separate the motion of the robot hand from that of the robot arm, which is usual in non-

redundant ones. Most researches for redundant robots, therefore, are focused on rigid-body robots.

In this work, a path of the flexible, redundant robot arm is designed to reduce the residual vibration of the arm tip in the presence of obstacles. First, a simple and effective dynamic model to ease the computation complexities both in motion and path analysis is established by using, so called, the VLCS (Virtual Link Coordinate System). Then, based upon this model, we optimize the path to reduce residual vibration in the presence of obstacles. A combined Fourier series and polynomial function is used after considering both the convergence and boundary condition matching problems. The concept of correlation coefficients is used to select the minimum number of design variables that only contribute to the reduction of residual vibration. Finally, the optimized path is tested on a planar, three-link manipulator to illustrate the effectiveness of the design of the path in reducing vibration.

2. DYNAMICAL MODELING

2.1. Generalized coordinates

The link flexibility can be represented as the deformation relative to the selected body-fixed coordinates. In general, we use the assumed spatial mode function to describe the deformation. This mode function, as is well-known, can vary largely depending on the selection of the coordinates.

As shown in Figure 1, link deformations are represented in two ways; One is with reference to the VLCS (a) and the other is relative to the tangent coordinate system (b). Both coordinate systems are moving coordinates, but the position of the former coordinate system is dependent only on joint angles of the preceding links. For instance, the origin of the VLCS for link 2 depends only on the angle θ_1, and is irrelevant to the deformation of link 1, as shown in Figure 1(a). In contrast, the origin of the tangent coordinate system $O_{2-x_2y_2}$ in Figure 1(b) depends not only on θ_1 but also on the deformation $v_1(L_1)$ of the preceding link deformation. In general, the motion of a tangent coordinate frame is a function of deformations $v_i(L_i)$ of the preceding links as well as the joint angles. That is why the equations of motion with respect to the tangent coordinate systems are coupled with the deformations of the other links. The VLCS, on the other hand, is independent of the deformations of the other links. Thus, the modeling by using the VLCS is an efficient way of formulating equations of motion in a compact form.

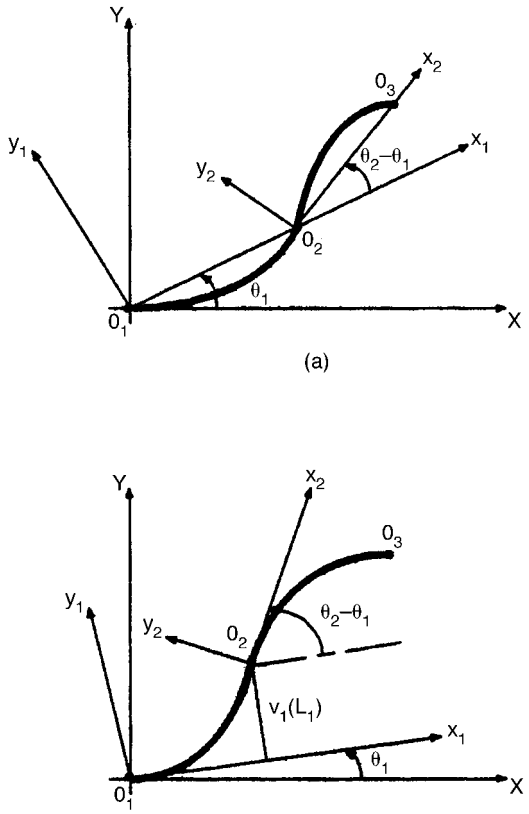

Fig. 1. Comparison of VLCS (a) and tangent coordinate system (b).

The mode functions to be used are dependent on the moving coordinates. When we adopt the tangent coordinate system as a moving coordinate, the mode functions used will be modes of a beam with one end fixed and the other free. This mode function has, as is well-known, a very complicated functional form. On the other hand, when we adopt the VLCS, we can use the mode functions of a simply-supported beam as an assumed mode function. This function is very simple and easy to handle.

As a result, the VLCS is not only convenient for solving the dynamical equation, but also advantageous to reduce computational complexity. The boundary conditions that the link beams must satisfy are much simpler when the beam deformations are represented with respect to the VLCS. Also this coordinate representation allows us to compute dynamic equations for each link member independently from the others. If one can use a system of orthogonal functions, the computation is further simplified, so that they can be divided into the ones in terms of individual generalized coordinate, separately.

2.2. Equations of motion

To formulate the dynamic equations of motion, we need to make assumptions on the construction of flexible arms discussed in this paper. We assume that the arm is planar, the open-loop linkage consisting of n links constrained in a horizontal plane.

In order to specify the configuration of a body, it is necessary to define a set of generalized coordinates. If we designate the axis $o_ix_iy_i$ as a coordinate system rigidly attached to i-th link and the axis $o_{i-1}x_{i-1}y_{i-1}$ to $(i-1)$-th link, the relative joint coordinates are specified by the relative angle θ_1 between the $o_{i-1}x_{i-1}y_{i-1}$ axis and the $o_ix_iy_i$ axis. In addition to the generalized coordinates above, one needs generalized coordinates associated with link deformation. To this end, we frst expand deformation $\boldsymbol{u}_i$ to a series of coordinates $\boldsymbol{q}_i^j$ by using the Rayleigh-Ritz functions for link i that satisfies conditions on independence and completeness, then the deformation $\boldsymbol{u}_i$ is written as

$$\boldsymbol{u}_i(x_i,t)=\sum_{j=1}^{s_i}\phi_i^j(x_i)\boldsymbol{q}_i^j \tag{1}$$

https://doi.org/10.1017/S0263574703005010 Published online by Cambridge University Press

In the above equation, ϕ_i^j is referred to as the assumed spatial mode function, and $\boldsymbol{q}_i^j$ as the time-varying mode amplitudes. Therefore, a vector of generalized coordinates of the i-th body is defined by the set of relative coordinates θ_i and modal coordinate $\boldsymbol{q}_i^j$.

Each joint of the manipulator is composed of an actuator, a transmission unit and an arm link. The elastic deformation of a joint is induced mainly by a transmission unit, because the elastic deformation of the gear teeth induces the joint flexibility. Therefore we model the joint flexibility as an equivalent torsional spring k_i, neglecting the inertia of the actuator.

The equation of motion of the physical system under consideration can be derived from the well-known Lagrangian equation. By substituting the kinetic energy, the potential energy and the generalized external force through tedious calculations, into the Lagrangian equation, we can derive the nonlinear differential equations of motion for the flexible, redundant manipulator.[17]

$$\boldsymbol{D}(\boldsymbol{X})\ddot{\boldsymbol{X}}+\boldsymbol{C}(\boldsymbol{X})\,\dot{\boldsymbol{X}}+\boldsymbol{K}\boldsymbol{X}+\boldsymbol{H}(\boldsymbol{X},\dot{\boldsymbol{X}})=\boldsymbol{T} \tag{2}$$

where $\boldsymbol{D}(\boldsymbol{X})$ is the time-varying inertia matrix, $\boldsymbol{C}$ and $\boldsymbol{H}$ represent the Coriolis, centrifugal, elastic and centrifugal stiffening effects. $\boldsymbol{K}$ is the stiffness matrix, and $\boldsymbol{T}=[\tau_1\ \tau_2\ \tau_3\ 0\cdots 0]^{\mathrm{T}}$ denote the generalized external vector. The generalized coordinate $\boldsymbol{X}$ is given by $\boldsymbol{X}=[\theta_1\ \theta_2\ \theta_3\ q_1^1\cdots q_1^{s1}\ q_2^1\cdots q_2^{s2}\ q_3^1\cdots q_3^{s3}]^{\mathrm{T}}$.

3. PATH OPTIMIZATION

3.1. Performance index

From the previous results,[12] the amplitude of the residual vibration can be minimized: both when the magnitudes of the error of the joint displacements and velocities at the final time is smaller, and when the ratio of these errors satisfies a certain criterion. Therefore, one cannot reduce the residual oscillations of the manipulator only by minimizing the absolute value of the final location error. In this paper the performance index to be minimized is chosen as the maximum value of the tip position error during the residual vibration:

$$J=Max\ p_e \quad (p_e=\sqrt{x_e^2+y_e^2} \quad \text{for } t\geq t_f) \tag{3}$$

The performance index in the above equation can be obtained by numerical integration of the equations of motion. Consequently, we need the dynamic equations derived in equation (2) to formulate the optimization problem.

The path constraints for obstacles take on the following form:

$$\mathrm{g_k(s)}=\psi_{\mathrm{k}}(\mathrm{s})-\ell_{\mathrm{k}}(\boldsymbol{r})<0 \quad k=1, 2, \ldots, p \tag{4}$$

where p is the number of the obstacles, s is a parameter to describe the path of the end-effector in workspace. $\boldsymbol{r}$ denotes a configuration of the manipulator and can be denoted as $\boldsymbol{r}\{\mathrm{x,y}\}$. $\psi_k(s)$ stands for the path equation of the tip, usually described as the displacement from the origin to the end-effector. $\ell_k(\boldsymbol{r})$ represent the location of the obstacles in work space.

3.2. Functional development of path

In order to formulate the optimal design problem, we need the functional development of each joint trajectory. Fourier and polynomial approximation techniques are commonly used in the functional expansion of generalized coordinates. A polynomial function exactly satisfies the boundary conditions, but contains the unwanted higher harmonics that excite the system resonance. Another demerit of this polynomial function is that we cannot assure the convergence of the solution by increasing the terms of the polynomials. On the other hand, a Fourier series expansion has the opposite characteristics: guarantees of convergence by adding terms and dissatisfactions of boundary conditions. So we propose the approximation method of each joint trajectory to combme the advantages of the two functions.

Any joint trajectory can be expanded by a finite cosine Fourier series using a half range expansion:

$$\theta_i(t)=a_{i0}+\sum_{m=1}^{M} a_{im}\cos\frac{m\pi}{t_f}t \tag{5}$$

This approach, however, has the following disadvantages:

(i) Convergence is guaranteed only in $(0, t_f)$. To satisfy the requirements on arbitrary conditions, convergence should be extended from $(0, t_f)$ to $[0, t_f]$.

(ii) Although $\theta_i(t)$ converges to the optimal solution, there is no guarantee that the derivative of $\theta_i(t)$ will converge to the derivative of the optimal solution.

(iii) The rate of convergence of the Fourier series depends on the optimal solution. This rate can be quite slow.

To overcome these disadvantages, we approximate each of the joint coordinates by the sum of a fifth order polynomial and a finite-term Fourier series.

$$\theta_i(t)=\lambda_i(t)+\sigma_i(t) \tag{6}$$

where

$$\lambda_i(t)=\sum_{j=0}^{5}\lambda_{ij}t^j \quad , \quad \sigma_i(t)=\sum_{m=1}^{M} a_{im}\cos\frac{m\pi}{t_f}t$$

Here, the constant term of the Fourier series has been included in the fifth-order polynomial, $\lambda_i(t)$.

The boundary condition requirements can be written as:

$$\begin{aligned}
&\theta_i(0)=\lambda_i(0)+\sigma_i(0)\\
&\theta_i(t_f)=\lambda_i(t_f)+\sigma_i(t_f)\\
&\dot{\theta}_i(0)=\dot{\lambda}_i(0)+\dot{\sigma}_i(0)\\
&\dot{\theta}_i(t_f)=\dot{\lambda}_i(t_f)+\dot{\sigma}_i(t_f)\\
&\ddot{\theta}_i(0)=\ddot{\lambda}_i(0)+\ddot{\sigma}_i(0)\\
&\ddot{\theta}_i(t_f)=\ddot{\lambda}_i(t_f)+\ddot{\sigma}_i(t_f)
\end{aligned} \tag{7}$$

These equations can be used to determine the coefficients of the polynomial in terms of the coefficients of the Fourier series and the boundary values. Solving the above boundary condition equations gives the following closed-form expression of the six coefficients:

$$\lambda_{ij}=\lambda_{ij}(a_{im}, \text{boundary value of } \theta_i,\ \dot{\theta}_i,\ \ddot{\theta}_i) \tag{8}$$

https://doi.org/10.1017/S0263574703005010 Published online by Cambridge University Press

Therefore, we can remedy the disadvantages of the Fourier series expansion, not increasing the number of terms to be designed. Also, the boundary conditions can be embedded naturally in the approximation to eliminate the kinetic requirements at both ends. The design variables are the coefficients of the Fourier series, $a_{im}(m=1, 2, \cdots, M)$.

If the design variables a_{im} are determined, the joint displacements, velocities and accelerations can be obtained by equation (6). Then the required torques to track the desired trajectory can be computed by the inverse dynamics. Applying these torques to the flexible dynamic equations, the dynamic responses of the flexible, redundant manipulator can be numerically obtained. From these results, we can compute the value of the performance index in equation (3). If this value cannot satisfy the optimality criterion, the optimization routine is iterated by adjusting the design variables a_{im} until the minimum point is reached.

3.3. Selection of design variables

In section 3.2, each joint trajectory was functionally developed by the combined polynomial and finite-term cosine Fourier series. But still the joint trajectories are expanded by all the sequential Fourier series up to the highest harmonic number. In that case, it is unavoidable that some Fourier coefficients which have a negligible contribution to the reduction of residual vibration are included in the expansion. Thus, if we take all the terms up to the highest harmonic number, the computation efficiency becomes worse. In general the accuracy of the optimal solution can be increased and its computing time can be greatly reduced, if we can remove the less contributing terms. For that reason, a technique to remove the less contributing terms in the combined Fourier series expansion is required.

The concept of correlation coefficients can be used to select the necessary Fourier terrns as follows. The correlation coefficients between the x position error of the arm tip, x_e and m-th harmonic function of Fourier series, $\sigma_m=\cos(m\,\pi\, t/t_f)$ are defined as follows:

$$\rho_{x_e\sigma_m}=\frac{S_{x_e\sigma_m}}{S_{x_ex_e}S_{\sigma_m\sigma_m}}=\frac{\sum_{k=1}^{N_d} x_e(k)\sigma_m(k)}{\sqrt{\sum_{k=1}^{N_d} x_e^2(k)\sum_{k=1}^{N_d}\sigma_m^2(k)}} \tag{9}$$

The correlation coefficients between the y position error and the m-th harmonic function, $\rho_{y_e\sigma_m}$ can be defined analogously. The correlation coefficient $\rho_{x_e\sigma_m}$ defined in equation (9) will lie between -1 and $+1$. And if the absolute value of it is in the vicinity of 1, it means that the correlation between x_e and σ_m is high and σ_m should be included in the expansion of the joint coordinates. In contrast, if the absolute value is near 0, σ_m can be excluded in the expansion.

$\rho_{x_e\sigma_m}$ has a different acceptance region according to the level of significance:

$$\frac{\sqrt{N_d-3}}{2}\left|\ln\left[\frac{1+\rho_{x_e\sigma_m}}{1-\rho_{x_e\sigma_m}}\right]\right|\geq z_{a/2} \tag{10}$$

where N_d is the number of the sampling data, z is the standardized normal variable, and, a is the level of significance. If $\rho_{x_e\sigma_m}$ satisfies the above inequality, we can say that a correlation exists between x_e and σ_m at the a level of significance. The same theory can be applied to $\rho_{y_e\sigma_m}$. Therefore, we can greatly reduce the number of design variables by selecting the harmonic functions satisfying the inequality (10) only.

4. RESULTS AND DISCUSSION

In order to analyze the dynamic response of the flexible, redundant manipulator, parameters such as mass, stiffness and Young's modulus must be provided. The arm construction we considered consists of rectangular aluminum beams of 1 (m) length each. The mass is 3.5 (kg), and the thickness is 1 (cm). The dimension of the cross section is 3×4 (cm), and Young's modulus is 7.1×10^3 (kgf/mm^2). The joint spring constant is 2(kN ·m/rad). The order of mode function is $s_1=s_2=s_3=3$ for each links. The duration time is 1 (sec). The manipulator starts its motion at $\theta_{10}=-90°$, $\theta_{20}=0°$, $\theta_{30}=-90°$; and ends at $\theta_{1f}=0°$, $\theta_{2f}=-45°$, $\theta_{30}=-45°$.

The motion of the arm tip is developed by cycloidal function and is shown in Figure 2. Cycloidal motion is one of the very smooth types of motion, largely used in the design of the cam profile. The actuator torques of the rigid manipulator required to track the desired trajectory can be found by the inverse dynamics. To evaluate the effects of the flexibility, a time series of computed torques are plugged into the flexible dynamic equations. The tracking errors and residual vibrations of the arm tip will be shown and discussed in later part of this chapter, compared with the optimized results.

Residual vibrations are composed of the tip position error in x and y direction. The correlation coefficients between the x and y position error of the arm tip for the cycloidal motion and the harmonic functions of the Fourier series are shown in Figure 3. If the number of data is 100, the correlation coefficients should be higher than 0.22 at the level of significance $a=0.01$ to satisfy equation (10). Only the fourth harmonic function in the x direction error, and the second, third and fourth in the y direction error satisfy this criterion. These harmonic numbers are equal to the variation of the first natural frequency of the system. Therefore the

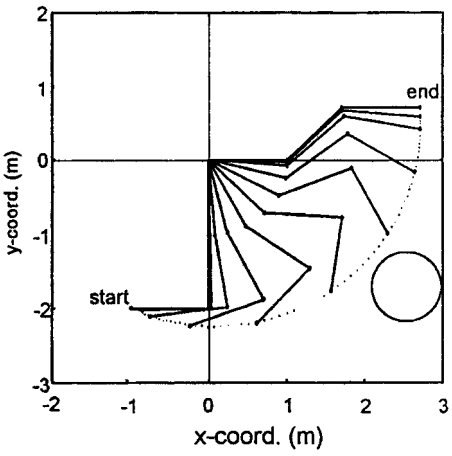

Fig. 2. Arm motion and tip path for cycloidal motion.

https://doi.org/10.1017/S0263574703005010 Published online by Cambridge University Press

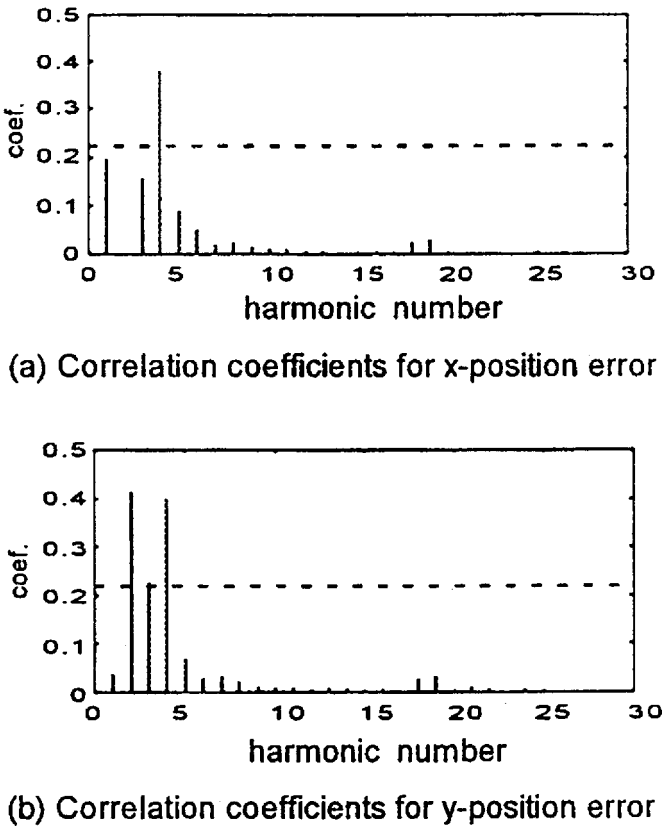

Fig. 3. Correlation coefficients of tip position error for cycloidal motion.

manipulator path can be developed by using only the 2,3 and 4-th harmonic functions of the Fourier series and polynomial function without serious errors.

The optimal path can be designed to reduce the residual vibration in the presence of the obstacles as we develop the path in functional form. The initial path is chosen as the cycloidal motion. The number of the obstacles is one and its location can be described as $\ell(x, y)=(x-2.6)^2+(y+1.7)^2-2.6^2$ in work space. The optimally designed paths are plotted in Figure 4 and Figure 5. Figure 4 represents the optimized path in the presence of the obstacle and Figure 5 does the one without obstacles constraints.

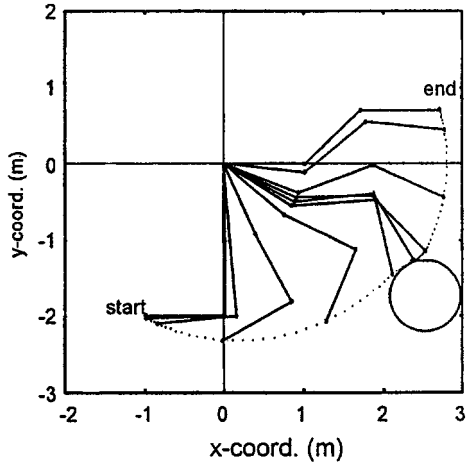

Fig. 4. Arm motion and tip path for optimized motion in the presence of obstacles.

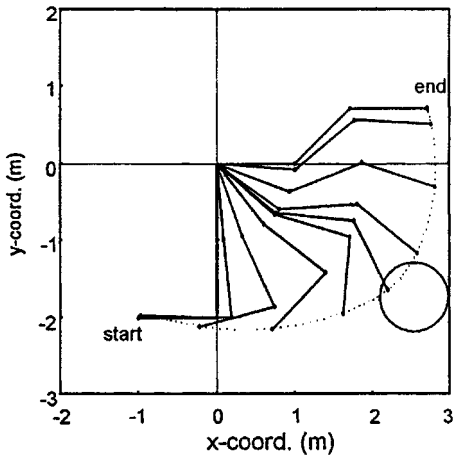

Fig. 5. Arm motion and tip path for optimized motion in the absence of obstacles.

At first, let us compare the path optimized without the obstacle constraints (Figure 5) with the cycloidal path (Figure 3). First of all, we can see that the tip moves more outwardly when it traces the optimized path. We can say from these results that Link 3 moves more outwardly relative to Link 2 in the optimized path. In other words, the joint angle between Link 2 and Link 3, θ_3, in the optimized path approaches more rapidly to final location than in the cycloid path. This means that the optimized path completes most of its motion faster, and then the arm tip approaches the final position compensating for the position errors caused by the fast motion. We can confirm these results from the optimized path in the presence of obstacles (Figure 4). As we can see from the figure, the arm tip tries to move outwardly but it cannot do because of the obstacles. So the arm tip moves toward the origin to avoid the obstacles, and then it moves outwardly again.

To evaluate the difference, the optimized path and computed torques are plugged into the dynamic equations. The tracking errors and residual vibration of the arm tip in the x, y directions are shown in Figure 6, in comparison with the response for cycloidal motion. As shown in the figure, the optimized path results in a very small residual vibration, while the cycloidal motion yields a relatively large vibration. The maximum amplitudes of the residual vibration are 5.63 (mm) in the x-direction and 17.01 (mm) in the y-direction for cycloidal motion, while it reduces to 3.15 (mm) in the x-direction and 7.64 (mm) in the y-direction for the path optimized in the presence of obstacles. These become lower when the tip traces the path optimized without obstacles constraint: 1.26 (mm) in the x-direction, 1.76 (mm) in the y-direction. The maximum amplitudes become significantly lower, only 55.9 and 22.4 percent of the maximum amplitude for the cycloidal motion in the x-direction, and only 44.9 and 10.3 percent in the y-direction.

The prominent frequency components of residual vibration for the cycloidal motion are 1.87 Hz and 8.65 Hz. The addition of the frequency components around the first frequency, 1.87 Hz, drastically reduces the magnitude of this frequency in the residual vibration for the optimized path. Physically, this means that the optimized path

https://doi.org/10.1017/S0263574703005010 Published online by Cambridge University Press

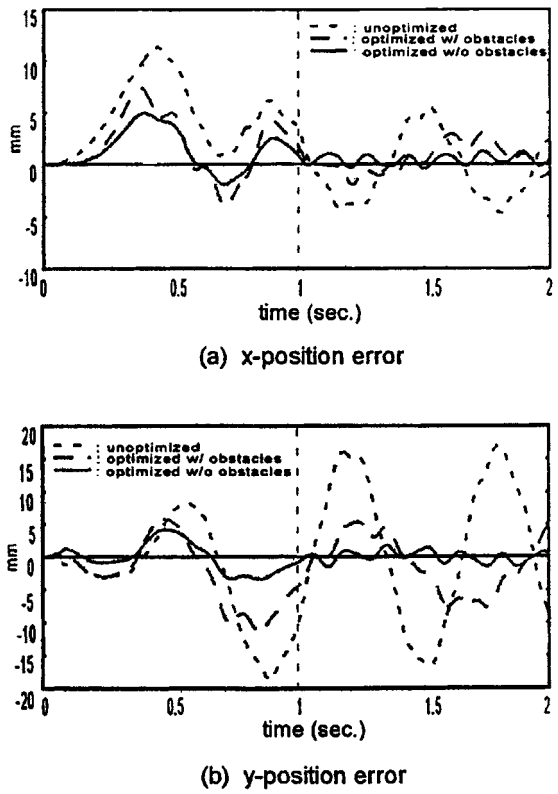

Fig. 6. Tip posiiion errors and residual vibration.

developed by the Fourier series (including these frequency components) offsets the occurrence of the oscillation with these frequencies. This fact can be assured by the results that the residual vibration in the y-direction, in which the first frequency component is more prominent, is largely reduced compared to the x-direction.

5. CONCLUSION

A method was presented for generating the path of a redundant flexible manipulator which significantly reduces residual vibration in the presence of obstacles. This is based on an optimized path that has been constructed from a combined Fourier series and polynomial, with coefficients of each harmonic term selected to minimize the residual vibration. In modeling the dynamics of a flexible arm, virtual link coordinates are used. These coordinates are not only convenient for modeling and optimization, but also advantageous for reducing computational complexity, especially for redundant flexible manipulators in which the number of links and joints increases additionally.

The manipulator path was developed by a combined Fourier series and polynomial. This expansion satisfies both the guarantees of convergence by adding terms and the matching of the boundary conditions. The concept of correlation was used to select the minimum number of design variables, i.e. Fourier coefficients, only contributing to the reduction of the residual vibration, which largely reduces the computing time.

The optimization algorithm has been applied to a 3-link planar redundant manipulator. Through simulation, the efficiency and usefulness of the optimized path were shown. Compared to a cycloidal motion, the optimized path produced motion with considerably lower residual vibration, even though obstacles were located along the path. From these results, it can be concluded that even in the presence of obstacles, the residual vibration of a redundant flexible manipulator could be drastically reduced by selecting an appropriate path.

References

1. R.F. Anthony and W.D. Ron, *Perturbation Techniques for Flexible Manipulator* (Kluwer Academic Publishers, Boston, USA, 1991).
2. W.J. Book, "Controlled Motion in an Elastic world", *ASME J. Dyn. Sys. Meas. Control* **115**(2), 252–261 (1993).
3. V.V. Karolov and Y.H. Chen, "Controller Design Robust to Frequency Variation in a One-Link Flexible Robot Arm", *ASME J. Dyn. Sys. Meas. Control* **111**(1), 9–14 (1989).
4. P. Meckl and W. Seering, "Active Damping in a Three-Axis Robotic Manipulator", *ASME J. Vib. Acou. Str. Relia. in Design* **107**(1), 38–46 (1985).
5. P. Meckl and W. Seering, "Minimizing Residual Vibration for Point-to-Point Motion", *ASME J. Vib. Acou. Stress Relia. in Design* **107**(3), 378–382 (1985).
6. W.E. Singhose, N.C. Singer and W.P. Seering, "Design and Implementation of Time-Optimal Negative Input Shapes", *Proc. Int. Mech. Eng. Cong.*, 151–157 (1994).
7. I. Yamada and M. Nakagawa, "Reduction of Residual Vibration in Position Control Mechanisms", *ASME J. Vib. Acou. Stress Relia. in Design* **107**(1), 47–52 (1985).
8. T.L. Vincent, S.P. Joshi and C.L. Yeong, "Positioning and Active Damping of Spring-Mass Systems", *ASME J. Dyn. Sys. Meas. Control* **111**(4), 592–599 (1989).
9. S. Jayasuriya and S. Choura, "On the Finite Settling Time and Residual Vibration Control of Flexible Robot Arm", *J. Sound and Vibration* **148**, 117–136 (1991).
10. O. William and L. Donogh, "Position Control of Flexible Robot Arms Using Mechanical Waves", *ASME J Dyn. Sys. Meas. Control* **120**(3), 334–339 (1998).
11. H. Asada, Z.D. Ma and H. Tokumaru, "Inverse Dynamics of Flexible Robot Arms: Modeling and Computation for Trajectory Control", *ASME J. Dyn. Sys. Meas. Control* **112**, 177–185 (1990).
12. K.J. Park and Y.S. Park, "Fourier-Based Optimal Design of a Flexible Manipulator Path to Reduce Residual Vibration of the Endpoint", *Robotica* **11**, 263–272 (1993).
13. K.J. Park and Y.S. Park, "Manipulator Path Design to Reduce the Endpoint Residual Vibration Under Torque Constraints", *Trans. KSME* **17**(10), 2437–2445 (in Korean, 1993).
14. C. Chevallereau, "Feasible Trajectories in a Task Space From a Singularity for a Non-Redundant or Redundant Robot Manipulator", *Int. J. Robotics Research* **17**(1), 56–69 (1998).
15. P.E. Dupont and S. Derby, "Two-Phase Path Planning for Robotics With Six or More Joints", *ASME J. Mechanical Design* **112**, 50–58 (1990).
16. M. Galicki, "The Planning of Robotic Optimal Motions in the Presence of Obstacles", *Int. J. Robotics Research* **17**(3), 248–259 (1998).
17. K.J. Park, "A Dynamic Approach to Motion Analysis for Flexible Redundant Robot Manipulators", *Bull. of Yosu Natl. Univ.* **11**(2), 393–401 (in Korean, 1998).

https://doi.org/10.1017/S0263574703005010 Published online by Cambridge University Press